Adipocyte Fatty Acid Transfer Supports Megakaryocyte Maturation

Colin Valet, Aurelie Batut, Alicia Vauclard, Alizee Dortignac, Marie Bellio, Bernard Payrastre, Philippe Valet, Sonia Severin

Adipocyte fatty acid transfer supports megakaryocyte maturation

Short title: adiposity and megakaryopoiesis

Colin Valet[1], Aurelie Batut[1], Alicia Vauclard[1], Alizee Dortignac[1], Marie Bellio[1], Bernard Payrastre[1,2], Philippe Valet[1] and Sonia Severin[1,*]

[1] *Inserm U1048 and Paul Sabatier University, Institute of Cardiovascular and Metabolic Diseases, Toulouse, France;*

[2] *Hematology Laboratory, Toulouse University Hospital*, *Toulouse, France;*

** Lead Contact: Sonia Severin, Inserm U1048 and Toulouse 3 University, I2MC, 31432 Toulouse Cedex 4, France. Phone: +33-531224143; Email: sonia.severin@inserm.fr*

Text word count: 32848 characters including spaces and figure legends
Summary word count: 145 words
Number of figures: 4

Keywords

Bone marrow; Adipocytes; Megakaryocytes; Fatty acids; Obesity

Summary

Megakaryocytes (MKs) come from a complex process of hematopoietic progenitor maturation within the bone marrow that give rise to *de novo* circulating platelets. Bone marrow microenvironment contains a large number of adipocytes with a still ill-defined role. This study aims to analyze the influence of adipocytes and increased medullar adiposity in megakaryopoiesis. An *in vivo* increased medullar adiposity in mice caused by high-fat-diet - induced obesity is associated to an enhanced MK maturation and proplatelet formation. *In vitro* co-culture of adipocytes with bone marrow hematopoietic progenitors shows that delipidation of adipocytes directly support MK maturation by enhancing polyploidization, amplifying demarcation membrane system and accelerating proplatelet formation. This direct cross-talk between adipocytes and MKs occurs through adipocyte fatty acid transfer to MKs involving CD36 to reinforce megakaryocytic maturation. Thus, these findings unveil an influence of adiposity on MK homeostasis based on a dialogue between adipocytes and MKs.

Introduction

Megakaryocytes (MKs) are highly specialized bone marrow (BM) cells releasing up to 10^{11} platelets on a daily basis in adult with a rapid turnover to maintain platelet homeostasis. MK maturation is a multi-step process where hematopoietic progenitors (HPs) increase in size, become highly polyploid (by endomitosis without cytokinesis), expand their organelle content and develop a dense membrane demarcation system (DMS), allowing proplatelet projections through medullary sinusoids at the origin of *de novo* circulating platelets (Machlus and Italiano, 2013; Machlus et al., 2014). This complex and ill-defined process of MK maturation mainly occurs in the BM under the control of thrombopoietin (TPO). Within central cavities of axial and long bones, BM consists of hematopoietic tissue islands and adipose cells surrounded by vascular sinuses (Travlos, 2006). BM adipose tissue constitutes 10% of the total fat body mass by filling 50%–70% of the bone cavity in healthy humans (Cawthorn et al., 2014; Hindorf et al., 2010) and increases in mass during metabolic modification conditions as aging, obesity or caloric restriction (Cawthorn et al., 2014; Doucette et al., 2015; Scheller et al., 2015). Considered for a long time as a passive "space fillers", BM adipocytes are specific adipocytes that share some morphological features with peripheral adipocytes but also present unique characteristics and functions (Attane et al., 2020; Cawthorn et al., 2014; Craft et al., 2018; Horowitz et al., 2017; Li et al., 2018; Scheller et al., 2016). It has been shown that BM adipocytes either in a steady state (Ambrosi et al., 2017; Naveiras et al., 2009) or under high-fat-diet (HFD)-induced obesity, where medullar adiposity increases, have an impact on general hematopoiesis by regulating hematopoietic stem and progenitor cells, lymphopoiesis and myelopoiesis, thymic aging and memory T cell maintenance (Adler et al., 2014a; do Carmo et al., 2013; Karlsson et al., 2010; Singer et al., 2014; Trottier et al., 2012; van den Berg et al., 2016; Yang et al., 2009). Considering the critical influence of adipocytes and adipose-rich BM for a normal hematopoiesis and the susceptibility of BM

microenvironment to obesity (Adler et al., 2014b; Asada et al., 2017), we addressed the question whether adipocytes and increased medullar adiposity could influence medullar megakaryopoiesis.

Results

Dysregulated medullar megakaryopoiesis, proplatelet formation and platelet activation in obese mice

To investigate whether a disturbed BM microenvironment with an increased adiposity could influence megakaryopoiesis, MK maturation was analyzed in a context of high-fat-diet (HFD)-induced obesity in mice (Figure S1A) where BM adiposity and triglyceride content increase (Figure 1A) (Doucette et al., 2015; Singer et al., 2014). Strikingly, we showed in obese mice that increased medullar adiposity correlates with a significant increase in total and nucleus size of medullar MKs without modifying their number (Figure 1B and Figure S1B). Polyploidy analysis (Figure S1C) of freshly isolated BM MKs showed an increased percentage of MKs with high ploidy levels in obese mice compared to normal diet (ND) -fed mice (Figure 1C). In contrast, obesity has no impact on extramedullary megakaryopoiesis as spleen size and splenic MK number and size were normal in obese mice (Figure S1D). We also observed that native BM MKs from obese mice displayed a large but poorly invaginated DMS (Figure 1D) and were able to elongate proplatelets faster than MKs from ND -fed mice (Figure 1E and Video S1-S2). Immunostaining of intact BM sections showed an increased proportion of MKs that extended proplatelets in obese mice compared to ND –fed mice. Also, the majority of proplatelet-forming MKs from obese mice extended proplatelets outside BM sinusoidal vessels (Figure 1F) and the proportion of CD41-positive (pro)platelet like particles outside BM sinusoidal vessels was increased in obese mice compared to ND -fed mice (Figure 1G).

Blood count analysis showed that murine obesity resulted in an increased monocyte count as previously described (Singer et al., 2014) and in a slightly decreased platelet count and increased platelet volume (Table S1). Following an immune-induced thrombocytopenia, we observed a delayed kinetic in platelet count recovery and a decreased *de novo* platelet release

in the circulation (Figure 1H). Circulating platelet clearance was increased in obese mice (Figure 1I). Transmission electron microscopy analysis of obese mice platelets did not highlight any obvious ultrastructure differences when compared to platelets from ND -fed mice (Figure S1E). Over a collagen matrix, platelets from obese mice display an increased thrombotic capacity compared to platelets from ND -fed mice, by forming bigger thrombi at a physiological arterial shear stress (1500 s-1) and even more at a stenotic arterial shear stress (3000 s-1) (Figure S1F). Tail bleeding time was however normal in obese mice (Figure S1G). Overall, these data indicate that a diet-induced obesity in mice, which increases medullar adiposity, modifies medullar MK homeostasis, circulating platelet release as well as platelet responses and clearance.

Adipocyte directly improves megakaryopoiesis

Since increased medullar adiposity in mice results in a modified megakaryopoiesis, we next analyzed if adipocytes could directly influence MK maturation. As only few MKs were in direct contact with adipocytes in the BM even with an increased adipose mass (Figure S2A), we set up an *in vitro* no-contact co-culture assay between adipocytes and freshly isolated mice BM hematopoietic progenitors (HPs) by using a transwell system in presence of TPO to commit HPs towards megakaryocytic maturation for 4 days (Figure S2B). Adipocytes were differentiated from mouse 3T3-F442A preadipocytes cell line or OP9 BM mesenchymal stem cells as shown by morphology changes with the appearance of lipid vacuoles and the increased expression of a specific adipocyte marker, adiponectin (Figure S2C and S2D). TPO itself had no impact on adipocyte differentiation (Figure S2E) and co-culture with HPs/MKs did not induce any adipocyte detachment or death (Figure S2F). We showed that adipocytes increased HPs/MKs survival with a higher proportion of cells negative for Annexin V in co-culture (Figure S2G) and significantly upregulated the proportion of cells expressing specific

fully differentiated MK markers (CD41 and CD42b) at their surface (Figure 2A). Moreover, larger cells were observed in the HP/MK population co-cultured with adipocytes (Figure S2H).

Polyploidy degree evaluation showed that adipocytes were able to dramatically enhance MK nuclear maturation through a non-physical contact process. Modal ploidy of mature MKs co-cultured with adipocytes was significantly higher than non-co-culture MKs, by resulting from a markedly increased proportion of MKs with ploidy levels equal or higher than 64n and a reduced percentage of MKs with lower ploidy levels (Figure 2B). Interestingly, one day of co-culture between adipocytes and HPs, either at an early or a late time point of MK differentiation process, was sufficient to significantly influence TPO-induced MK polyploidization (Figure S2I). It is noteworthy that the positive effect of adipocytes on MK nuclear maturation amplification was also observed in absence of TPO (Figure S2J). By transmission electron microscopy, we observed bigger MKs with a fragmented, discontinuous and less structured DMS in MKs co-cultured with adipocytes compared to non-co-cultured MKs where DMS is mainly concentrated in one side of the cell (Figure 2C). This abnormal DMS from MKs in co-culture with adipocytes was associated to an increased proportion of MKs forming proplatelets (Figure 2D). The enhanced CD41/CD42b expression, MK polyploidization and proplatelet formation induced by adipocytes was not observed with non-differentiated 3T3-F442A or OP9 cells (Figure S3) confirming a specific effect of lipid-filled fully differentiated adipocytes on megakaryopoiesis.

Following TPO binding, c-MPL dimerizes and induces janus kinase 2 (JAK2) autophosphorylation leading to the activation of signal transducers and activators of transcription (STATs), mitogen-activated protein kinases (MAPKs) and phosphoinositide 3-kinases (PI3Ks) (Geddis, 2010). In co-culture with adipocytes in presence of TPO, we observed a significantly increased phosphorylation of JAK2, STAT3, AKT and MAPK

ERK1/2 (Figure 2E), showing an enhanced activation level of signaling pathways involved in MK differentiation in the presence of adipocytes.

MKs are responsible for adipocyte delipidation

Interestingly, we observed that after 4 days of co-culture with HPs/MKs, adipocytes exhibited a significant reduction in their lipid droplet content (Figure 3A) and triglyceride content (Figure 3B). Surprisingly, MK supernatant was able to induce a significant delipidation of adipocytes (Figure 3C). This adipocyte lipolysis in presence of MK supernatant, occurring at a similar extent than the co-culture between adipocytes and MKs, showed that MK constitutive releasate influences adipocyte homeostasis. Mechanistically, co-cultured adipocytes displayed an increased phosphorylation level of the hormone-sensitive lipase (HSL) on its serine 660 residue (Figure 3D) that promotes its activation for adipocyte delipidation (Fruhbeck et al., 2014; Nielsen et al., 2014) and a decreased expression of adipocyte specific markers such as PPARγ, aP2 and adiponectin (Figure 3E). The increased CFU-F capacities of co-culture 3T3-F442A and OP9 –cells (Figure 3F) and the fact that these cells were able to re-commit in adipocytes (Figure 3G) provided further evidence that MKs induce a delipidation of 3T3-F442A and OP9 –differentiated adipocytes. Thus, co-culture of adipocytes with HPs/MKs induce adipocyte lipolysis through HSL signaling pathway activation.

MKs uptake fatty acid released by adipocytes *via* the CD36 scavenger receptor to improve their maturation

We further addressed how adipocytes could influence MK maturation. For that, we analyzed MK maturation after incubating HPs with adipocyte supernatant or with co-culture supernatant in presence of TPO. We observed that adipocyte supernatant increased the

polyploidy levels of MKs (Figure 4A and Figure S4A). This enhancement was further increased when MKs were differentiated into the co-culture supernatant (Figure 4A and Figure S4A), showing that HPs/MKs-induced adipocyte release enhances MK maturation.

Adipocytes have been shown to secrete TPO, the main cytokine for megakaryopoiesis (Ge et al., 2011). We observed that co-culture with MKs decreased TPO mRNA level in adipocytes, (Figure S4B). The decreased TPO mRNA expression in adipocytes co-cultured with MKs (Figure S4B) and the lack of effect of the blocking anti-TPO antibody on adipocytes enhanced MK polyploidization (Figure S4C) led to conclude that adipocyte-secreted TPO was not the causative factor for the increased megakaryopoiesis. Interestingly, when HPs/MKs were co-cultured with ^{14}C palmitate-labeled adipocytes, we detected ^{14}C palmitate in mature MKs (Figure 4B) associated to a decreased proportion of ^{14}C palmitate in co-cultured adipocytes and a higher concentration of the radiolabeled fatty acid in the co-culture supernatant (Figure 4B). The ^{14}C palmitate transferred from adipocytes to MKs was detected in MK neutral lipids and phospholipids (Figure 4B). Altogether, our data demonstrate that HPs/MKs stimulate adipocyte release of fatty acids that are directly uptaken by MKs.

We further investigated the mechanisms by which fatty acid uptake by MKs influences their maturation. HPs were co-cultured with adipocytes in presence of the sulfo-N-succinimidyl oleate (SSO) that has been widely used to irreversibly inhibit the plasma membrane fatty acid translocase CD36 (Coort et al., 2002). Whereas SSO treatment had no effect on non-co-cultured MK nuclear maturation (Figure S5A), we observed that inhibiting CD36 significantly reduced MK maturation enhancement induced by adipocytes to a non-co-cultured MK maturation level (Figure 4C and Figure S5B). The abnormal MK DMS ultrastructure induced by adipocyte co-culture was also counteracted by SSO treatment during MK differentiation with the DMS localized in one side of MKs (Figure 4D). Moreover, whereas an acute SSO treatment of MKs after co-culture with adipocytes had no effect on MK proplatelet formation

(Figure S5C), SSO treatment along MK differentiation process restored the percentage of MKs forming proplatelets to a level comparable to non-co-cultured MK level (Figure 4E). These findings demonstrate that the CD36-dependent fatty acid uptake by MKs directly improves MK maturation and proplatelet formation. Nevertheless, inhibiting the entry of fatty acids into mitochondria for β-oxydation with etomoxir had no consequences on MK polyploidization (Figure S5A and S5D) or on proplatelet formation when MK are co-cultured with adipocytes (Figure S5E). Thus, these data exclude the energetic contribution of the CD36-dependent lipid uptake on MK maturation.

We further observed that adding palmitic acid on HPs during TPO-induced megakaryocytic differentiation increased MK size (Figure S5F) and improved MK nuclear maturation (Figure 4F and Figure S5G). Phosphorylation of proteins involved in MK maturation-dependent signaling was significantly increased in MKs differentiated in presence of palmitic acid (Figure 4G). Furthermore, when fluorescent fatty acid Bodipy^{TM} C12-loaded adipocytes (from 3T3-F442 or OP9 cells) were co-cultured with HPs/MKs, fluorescent fatty acids were found in the DMS and at the plasma membrane of mature MKs as assessed by the colocalization of fluorescent fatty acids with the $DIOC_6$ membrane marker (Figure 4H). The absence of Bodipy^{TM} C12 staining in MKs co-cultured with Bodipy^{TM} C12-loaded adipocytes and SSO or in MKs co-cultured with Bodipy^{TM} C12-loaded non-differentiated 3T3-F442A or OP9 confirmed that fatty acids released by adipocytes were the source of lipids for MKs through uptake by CD36 (Figure 4H and Figure S5H). In line with these results, addition of palmitic acid disturbed DMS structure (Figure 4I) and increased the proportion of MKs extending proplatelets (Figure 4J). Altogether, these results showed that adipocyte-derived fatty acids contribute directly to polyploidization, development of MK DMS and therefore to proplatelet formation.

Discussion

Although the analysis of megakaryopoiesis have been the interest of several laboratories since many years, elucidating the molecular and cellular events involved in this process remains an unfinished task. As adipocytes are a major component of the medullar niche homeostasis, we investigated whether they could influence MK biology. Due to the weak proportion of MKs in direct contact with the BM adipocytes, we investigated the paracrine adipocyte/MK communication independent of cell-cell contact by using an *in vitro* no-contact co-culture assay. We clearly demonstrate that adipocytes strongly influence MK maturation that involved a direct dialogue between HPs/MKs and adipocytes. In one hand, adipocytes support HP survival and enhance their differentiation into the MK lineage by heightening MK polyploidy, modifying MK membrane structure and accelerating proplatelet formation. In the other hand, HPs/MKs induced adipocyte delipidation. Our results also shed light that the initiating event of the crosstalk between adipocytes and MKs remains the MK ability to release soluble factors to modify adipocyte homeostasis by inducing its delipidation, which in turn favors the proper MK differentiation. In line with these results, MKs have been also shown to influence the BM matrix reorganization and the homeostasis of endothelial cells, osteoblasts/osteoclasts hematopoietic cells within the BM by releasing soluble factors such as cytokines, extracellular matrix (ECM) components and metalloproteinases (Bonner, 2004; Chagraoui et al., 2002; Guerrero et al., 2014; Malara et al., 2015; Malara et al., 2018; Malara et al., 2014; Pohlers et al., 2009; Wickenhauser et al., 1995).

Adipocyte canonical function is to store energy as triglycerides for releasing fatty acids to metabolic tissue utilization. Our study shows a crosstalk between adipocytes and MKs through a direct fatty acid transfer from adipocytes to MKs that is dependent of the fatty acid translocase CD36 known to be expressed at the surface of MKs (Coort et al., 2002; Pepino et al., 2014). In line with previous studies (Dhenge et al., 2017; Murphy et al., 2013; Siddiqui et

al., 2011), we clearly point out that fatty acids can directly influence megakaryopoiesis by enhancing ploidy levels of MKs through the regulation of MK maturation related-signaling pathways. We also show that fatty acids released by adipocytes are a source of structural lipids for DMS amplification. As SSO has an impact on proplatelet formation only when it is present during MK differentiation process (i.e when MK differentiation is enhanced by adipocytes), we conclude that the increased proplatelet formation of MKs co-cultured with adipocytes is a direct consequence of the increased nuclear and cytoplasmic/membrane differentiation induced by adipocyte fatty acid uptake by MKs. A close communication between adipocytes and cancer cells *via* a fatty acid release by adipocytes has also been previously reported (Laurent et al., 2019; Nieman et al., 2011; Wang et al., 2017). However, whereas the fatty acid transfer from adipocytes to cancer cells occurs in an energetic way through mitochondrial fatty acid oxydation, it is not the case for the adipocyte lipid transfer in MKs.

In the settlement of obesity, BM environment undergoes considerable changes such as hyperplasia with a ~20–30% increased marrow cellularity, increased adiposity and modifications of growth factor/cytokine secretion, conditions that disrupt chemical, physical and cellular connections of the BM. Literature also shed the light on the role of adipocytes and obesity on the regulation of long term hematopoietic stem and progenitors cells, lymphopoiesis and myelopoiesis (Adler et al., 2014a; do Carmo et al., 2013; Karlsson et al., 2010; Singer et al., 2014; Trottier et al., 2012; van den Berg et al., 2016; Yang et al., 2009). In addition to these data, our *in vitro* co-culture assay clearly showed an important influence of adipocytes on megakaryopoiesis and that obesity with an increased medullar adiposity modified the MK phenotype as observed *in vitro*. Systemic changes such as global metabolism dysregulation and chronic low-grade inflammation changes could influence megakaryopoiesis in addition to the increased medullar adiposity. Nevertheless, the lack of

influence of obesity on splenic megakaryopoiesis where adipocytes are absent, strongly argues for a determinant role of increased medullar adiposity on the modified medullar megakaryopoiesis.

The functional importance of the crosstalk between MKs and adipocytes might contribute to a better understanding of the altered thrombosis and hemostasis status observed in the obese population. The non-stretchable compartment of the BM, in which adiposity and MK mass increased, might prevent large MKs from reaching the sinusoids and is likely responsible for platelet presence outside the BM vasculature and decreased circulating platelet count. Obesity also enhanced the clearance of platelets and their thrombotic reactivity. Even if the low-grade inflammation of the obesity might directly impact on platelets, the influence of adipocytes and obesity on MK homeostasis could directly modify the intrinsic characteristics of platelets that impact on their reactivity. This is illustrated by a recent study from Di Paola laboratory showing that aging, which induces metabolic changes similarly to obesity, are responsible for MK gene reprogramming and metabolic profile changes that determine platelet hyperactivity in old mice (Davizon-Castillo et al., 2019).

Therefore, our study provides insights on how the cellular medullary microenvironment supports megakaryopoiesis and contributes to the growing list of marrow cellularity dysregulation known to be associated to obesity. Considering the limitations of the study several questions remain open: Does the MK/adipocytes communication in BM from obese mice involve others factors (as chemokines/cytokines resulting from the systemic changes associated to obesity) in addition to the fatty acid transfer we characterized in our *in vitro* co-culture? Do platelets arising from bigger MKs display distinct lipid, gene and metabolic profiles responsible for intrinsic changes in platelet reactivity and clearance? Do BM adipocytes dedifferentiate or only delipidate via an HLS-dependent lipolysis? What are the molecule(s) released by MKs susceptible to influence adipocyte homeostasis?

Acknowledgements

We thank the personnel of Anexplo animal facilities (UMS US006/ Inserm) for animal handling, of experimental histopathology of UMS US006/ Inserm (F. Capilla), of Cytometry core facility of Inserm UMR1048 (E. Riant and A. Zakaroff-Girard), Genotoul imaging core facility (Inserm UMR1048, E. Vega and R. Flores-Flores and CMEAB, I. Fourquaux) and of MetaToul-Lipidomic core facility of Inserm U1048 (J. Bertrand-Michel). The authors thank all members from the B.P. and P.V laboratories and A. Mairal for helpful discussions. C.V. was supported by fellowships from Université Paul Sabatier and Société Francaise d'Hématologie. M.B. was supported by a Fondation pour la Recherche Médicale fellowship (FRM grant number ECO20160736022 [MB]). A.V. was supported by Fondation de France (grant number 00075817 [SS]). Work in B.P. laboratory was supported by Inserm, Fondation pour la Recherche Médicale (FRM grant number DEQ20170336737 [BP]) and Fondation de France (grant number 00075817 [SS]). B.P. is a scholar of the Institut Universitaire de France. Work in P.V. laboratory was supported by Inserm and the Fondation pour la Recherche Médicale (FRM grant number ING20121226373 [PV]).

Authorship contributions

Conceptualization – C.V., P.V., B.P., S.S.; Methodology – C.V., S.S.; Validation – S.S.; Investigation – C.V., A.B., A.V., A.D., M.B., S.S.; Writing – Original Draft, C.V., A.V., S.S.; Writing – Review & Editing – P.V., B.P.; Visualization – C.V., A.B., A.V., M.B., S.S.; Funding Acquisition – S.S.; Supervision and Project Administration – S.S.

Declaration of Interests

The authors declare no competing interests.

Figure Legends

Figure 1. Dysregulated medullar megakaryopoiesis, proplatelet formation and platelet activation in obese mice

(**A**) Representative images of mice bone marrow (BM) hematoxylin/eosin staining. The entire tibiae (scale bar: 1mm) and a zoomed region of the diaphysis (scale bar: 250µm) are shown. Adipocytes are mentioned by arrows. Graph represents triglyceride content of the total BM and is mean±SD of 6 mice of each genotype (**p<0.01 versus ND -fed mice according to two-tailed Student t test)

(**B**) Zoom region of mice tibiae diaphysis stained with hematoxylin/eosin. Scale bar: 50µm. MKs are mentioned by arrows. Number of MKs per mm², mean MK total area and nucleus area were manually quantified by using NDPview software (mean±SD; n=350 MKs from 4 mice of each genotype; ***p<0.001 versus ND -fed mice according to two-tailed Student t test).

(**C**) Polyploidy analysis of native BM MKs assessed by propidium iodide staining and flow cytometry. Representative panels and quantification of the percentage of cells with different levels of ploidy are shown (mean±SD; n=4 mice of each group; ***p<0.001 versus ND -fed mice according to two-way ANOVA).

(**D**) Representative transmission electron microscopy images of native MKs from BM sections. Scale bar: 5µm (non-zoomed images) and 0.5µm (zoomed images). MK DMS percent occupancy was manually measured by using ImageJ® software (mean±SD; n=4 mice of each group; ***p<0.001 versus ND -fed mice according to two-tailed Student t test).

(**E**) Proplatelet formation analysis from native MKs from BM explants. Representative images of MKs forming proplatelets are shown. Scale bar: 50µm. The percentage of MKs extending proplatelets at different time point was quantified by using Zen software

(mean±SD; n=50 MKs from 3 mice of each genotype; *p<0.05, **p<0.01 versus ND -fed mice according to two-way ANOVA).

(**F**) Representative confocal images of cryoconserved immunostained native BM of mice tibiae. MKs, sinusoid vessels and nucleus were respectively stained for vWF (green), for FABP-4/A-FABP (delineated in white) and with 4′,6-diamidino-2-phenylindole (blue). Scale bar: 50µm (non-zoomed images) and 8µm (zoomed images). Proplatelet-forming MKs are mentioned by arrows. Zoomed images are mentioned by squares. The graph represents the percentage of round MKs "A", MKs forming proplatelets inside vessels "B", and MKs forming proplatelets outside vessels "C" (mean±SD; n=30 images from 3 mice of each genotype, ***p<0.001 versus ND -fed mice according to two-way ANOVA).

(**G**) Percentages of CD41-positive particles inside and outside sinusoids quantified on confocal images of cryoconserved immunostained native BM of mice tibiae (mean±SD; n=30 images from 3 mice of each genotype, *p<0.05 versus ND -fed mice according to two-way ANOVA).

(**H**) Platelet count recovery after immune-induced thrombocytopenia evaluated in blood samples (mean±SD; n=4 mice; *p<0.05, **p<0.01, ***p<0.001 versus ND -fed mice according to two-way ANOVA).

(**I**) Platelet clearance evaluated by quantifying the percentage of Dylight^{488}-anti-GPIbβ Ig derivative labeled platelets (mean±SD; n=4 mice; **p<0.01, ***p<0.001 versus ND -fed mice according to two-way ANOVA).

ND: normal diet; HFD: high-fat-diet.

See also Figure S1, Video S1, Video S2.

Figure 2. Adipocyte directly improves megakaryopoiesis.

(**A**) CD41/CD42b surface expression analyzed in alive HP/MK population after co-culture with 3T3-F442A or OP9 -differentiated adipocytes for 4 days in presence of TPO (mean±SD; n=5 independent experiments; $**p<0.01$, $***p<0.001$ versus MK according to one-way ANOVA).

(**B**) Representative MK ploidy degree panels and quantitative analysis of the percentage of cells with different levels of ploidy and of modal ploidy (mean±SD; n=11 and 10 independent experiments respectively for 3T3-F442A and OP9; $*p<0.05$, $**p<0.01$, $***p<0.001$ versus MK according to two-way ANOVA and two-tailed Student *t* test).

(**C**) Representative transmission electron microscopy images (from 30 MKs from 3 independent experiments) of MKs co-cultured or not with adipocytes after BSA gradient isolation. Scale bar: 10µm.

(**D**) Proplatelet formation of MKs analyzed after 6 hours plating on a fibrinogen surface. Representative transmission images of MKs forming proplatelets are shown by using the ZOE™ Fluorescent Cell Imager. MKs forming proplatelet are mentioned by arrow. Scale bar: 100µm. The graph represents the percentage of MKs forming proplatelets (mean±SD; n=3 independent experiments; $***p<0.001$ versus MK according to one-way ANOVA).

(**E**) MKs isolated from BSA gradient were lysed and protein samples were immunoblotted using specific antibodies: anti-pJAK2 (Tyr1007/1008), anti-pSTAT3 (Tyr705), anti-pAKT (Ser473), anti-pERK (Thr202/Tyr204). Total JAK2, STAT3, AKT, ERK1/2 and GAPDH were used as control loading. Representative western blots are shown and the ratio phosphorylated/total of each protein was quantified using ImageLab software. Graphs represent fold increase phosphorylation in comparison to non-co-cultured MKs as mean±SD (n=3 and 4 independent experiments for 3T3-F442A and OP9 respectively; $*p<0.05$, $**p<0.01$, $***p<0.001$ versus MK according to one sample *t* test).

MK: HPs/MKs cultured alone; MK/3T3: HPs/MKs co-cultured with 3T3-F442A -differentiated adipocytes; MK/OP9: HPs/MKs co-cultured with OP9 -differentiated adipocytes.

See also Figure S2, S3 and S6.

Figure 3. MKs induced adipocyte delipidation.

(**A**) Red oil representative images and labeling quantification of 3T3-F442A or OP9 -differentiated adipocytes co-cultured or not with MKs in presence of TPO for 4 days. Scale bar: 100µm. The graph represents the percent of Red oil labeling per field (mean±SD; n=3 independent experiments; ***p<0.001 versus 3T3 or OP9 according to two-tailed Student t test).

(**B**) Triglyceride content quantified in adipocytes after co-culture or not with MKs (mean±SD; n≥5 independent experiments; *p<0.05, **p<0.01 versus 3T3 or OP9 according to two-tailed Student t test).

(**C**) Adipocytes were cultured in control medium or in HP/MK supernatant (MK SN) for 4 days in presence of TPO and triglyceride content was quantified (mean±SD; n=5 independent experiments; *p<0.05 versus 3T3 or OP9 according to two-tailed Student t test).

(**D**) After co-culture or not with MKs, adipocytes were lysed and protein samples were analyzed by immunoblotting using the pHSL (Ser660) specific antibody. HSL and Actin were used as loading controls. Representative western blots are shown and quantification was represented as mean±SD (n=9 and 4 independent experiments for 3T3 and for OP9 respectively; *p<0.01 versus 3T3 or OP9 according to one sample t test).

(**E**) PPARγ, aP2 and adiponectin mRNA expression quantified in adipocytes co-cultured or not with MKs (mean±SD; n=5 independent experiments; *p<0.05, **p<0.01, ***p<0.001 versus 3T3 or OP9 according to two-tailed Student t test).

(**F**) Number of CFU-Fibroblast (CFU-F) manually quantified on 25cm² flasks from 3T3-F442A or OP9 cells in a non-differentiated status (3T3 non-diff or OP9 non-diff), non-co-culture 3T3-F442A or OP9 -derived adipocytes (3T3 or OP9) or 3T3-F442A or OP9 -derived adipocytes co-cultured with MKs (3T3/MK or OP9/MK) (mean±SD; n=6 independent experiments, $**p<0.01$, $***p<0.001$ according to one-way ANOVA).

(**G**) Capacity of CFU-F from (F) to recommit to adipocytes. Representative transmission images before and after adipogenic differentiation are shown (n=6 independent experiments) by using the ZOE™ Fluorescent Cell Imager. Scale bar: 100µm.

3T3: 3T3-F442A -differentiated adipocytes; 3T3 non-diff: non-differentiated 3T3-F442A; 3T3/MK: 3T3-F442A -differentiated adipocytes co-cultured with HPs/MKs; 3T3/MK SN: 3T3-F442A -differentiated adipocytes cultured with HP/MK supernatant; OP9: OP9 -differentiated adipocytes; OP9 non-diff: non-differentiated OP9; OP9/MK: OP9 -differentiated adipocytes co-cultured with HPs/MKs; OP9/MK SN: OP9 -differentiated adipocytes cultured with HP/MK supernatant.

See also Figure S6.

Figure 4. The CD36- fatty acid uptake by MKs is essential to improve their maturation.

(**A**) HPs/MKs were cultured with 3T3-F442A or OP9 -differentiated adipocyte supernatant (3T3 SN or OP9 SN) or adipocyte/HP/MK co-culture supernatant (co-culture SN). MK DNA ploidy was analyzed by flow cytometry after propidium iodide labeling (mean±SD; n=4 independent experiments; $*p<0.01$, $**p<0.01$, $***p<0.001$ according to two-way ANOVA).

(**B**) C^{14} palmitate labeled 3T3-F442A or OP9 -differentiated adipocytes were co-cultured or not with HPs/MKs. Radioactivity in adipocytes, MKs and supernatant was quantified (mean±SD; n=4 independent experiments; $*p<0.05$, $**p<0.01$, $***p<0.001$ versus 3T3 or OP9 according to two-way ANOVA). The presence of C^{14} palmitate was quantified in neutral

lipids (NL) and different phospholipids (PC: phosphatidylcholine, PE: phosphatidylethanolamine, PI: phosphatidylinositol, PS: phosphatidylserine) as described in Methods.

(**C-E**) HPs/MKs were cultured in normal medium with DMSO (MK+vehicle), in adipocyte/MK co-culture supernatant with DMSO (MK/3T3+vehicle or OP9/MK+vehicle) or in adipocyte/MK co-culture supernatant with sulfo-N-succinimidyl oleate (SSO) (200µM) (MK/3T3+SSO or OP9/MK+SSO). (**C**) MK DNA ploidy quantified as the percentage of cells with different levels of ploidy equal or greater to 8n (mean±SD; n= 3 independent experiments; *p<0.05, **p<0.01, ***p<0.001 according to two-way ANOVA); (**D**) Representative transmission electron microscopy images of MKs. Scale bar: 10µm; (**E**) Proportion of MKs forming proplatelet formation after 6 hours plating on a fibrinogen surface (mean±SD; n=3 independent experiments; **p<0.01, ***p<0.001 according to one-way ANOVA).

(**F-G**) 2.10^6 HPs were cultured in presence of TPO for 4 days with ethanol (vehicle, V) or with palmitic acid (PA) (250µM). (**F**) MK ploidy quantified as the percentage of cells with different levels of ploidy equal or greater to 8n (mean±SD; n=4 independent experiments; **p<0.01, ***p<0.001 versus vehicle according to two-way ANOVA); (**G**) MK were lysed and protein samples were immunoblotted using specific antibodies: anti-pJAK2 (Tyr1007/1008), anti-pSTAT3 (Ty705), anti-pAKT (Ser473), anti-pERK (Thr202/Tyr204). Total JAK2, STAT3, AKT, ERK1/2 and GAPDH were used as control loading. Representative western blots are shown and the ratio phosphorylated/total of each protein was quantified using ImageLab software. Graphs represent fold increase phosphorylation in comparison to MKs with vehicle as mean±SD (n=7 independent experiments; *p<0.05, **p<0.01 versus vehicle according to one sample t test).

(**H**) Bodipy^{TM} C12-labeled adipocytes were co-cultured with HPs/MKs and TPO for 4 days with vehicle or SSO (200µM) were analyzed by confocal microscopy. Representative confocal images of Bodipy^{TM} C12 and $DIOC_6$ labeled- MKs from 3 independent experiments. Scale bar: 10µm.

(**I-J**) HPs/MKs were cultured for 4 days in presence of TPO with ethanol (vehicle) or with palmitic acid (250µM). (**I**) Representative transmission electron microscopy images from 3 independent experiments was taken. Scale bar: 10µm; (**J**) Proportion of MKs forming proplatelets after 6 hours plating on a fibrinogen surface (mean±SD; n=3 independent experiments; ***p<0.001 versus vehicle according to two-tailed Student t test).

MK: HPs/MKs cultured alone; MK+3T3 SN: HPs/MKs cultured with 3T3-F442A -differentiated adipocyte supernatant; MK/3T3+vehicle: HPs/MKs cultured with 3T3-F442A -differentiated adipocyte supernatant with DMSO; MK/3T3+SSO: HPs/MKs cultured with 3T3-F442A -differentiated adipocyte supernatant with SSO; MK+OP9 SN: HPs/MKs cultured with OP9 -differentiated adipocyte supernatant; MK+co-culture SN: HPs/MKs cultured in supernatant of co-culture; MK/OP9+vehicle: HPs/MKs cultured with OP9 -differentiated adipocyte supernatant with DMSO; MK/OP9+SSO: HPs/MKs cultured with OP9 -differentiated adipocyte supernatant with SSO.

See also Figure S4, S5 and S6.

STAR Methods

LEAD CONTACT

Further information and requests for resources and reagents should be directed to and will be fulfilled by the Lead Contact, Dr Sonia Severin (sonia.severin@inserm.fr).

MATERIALS AVAILABILITY

This study did not generate new unique reagents.

DATA AND CODE AVAILABILITY

This study did not generate any unique datasets or code.

EXPERIMENTAL MODEL AND SUBJECT DETAILS

Animals: All C57BL/6J mice were purchased from Janvier Labs and were backcrossed in house. Mice were housed in conventional cages under specific pathogen-free conditions in a constant temperature (20–22°C) and humidity (50–60%) animal room with a 12/12 h light/dark cycle (lights on at 7:00 AM) and free access to food and water. To isolate HPs, male mice were used at 10-20 weeks old. To induce obesity, male mice were fed at 8 weeks aged (when mice are considered to be adult) with a high-fat-diet (HFD: 20% protein, 20% carbohydrate, 60% fat) (ResearchDiets, NJ, US) for 12 weeks. Normal diet (ND) is composed of 24% protein, 67% carbohydrate, 9% fat (Ssniff, Germany). All procedures were performed in accordance with institutional guidelines for animal research and were approved by the French Ministry of Research in agreement with European Union guidelines.

Differentiation into adipocytes: Mouse 3T3-F442A pre-adipocyte cells and mouse OP9 BM mesenchymal stem cells were purchased from commercial vendors noted in the Key Resources Table. Adherent mouse 3T3-F442A cells were set to adhere and growth in growth enhanced-treated TPP tissue culture Testplate 6 wells (TPP®) in DMEM Glutamax™ (Invitrogen) supplemented with 10% fetal bovine serum (Invitrogen) and 100UI/mL penicillin/100µg/mL streptomycin (Sigma-Aldrich) at 37°C under 5% CO_2. At confluence, 3T3-F442A cells were differentiated into DMEM Glutamax™ supplemented with 10% fetal bovine serum and 100UI/mL penicillin/100µg/mL streptomycin in presence of 50nM insulin (Sigma-Aldrich) for 7 days at 37°C under 5% CO_2 (Boucher et al., 2005). Adherent OP9 cells were growth in MEMα Medium Glutamax™ (Invitrogen) supplemented with 20% fetal bovine serum and 100UI/mL penicillin/100µg/mL streptomycin in Nunclon™ Delta Surface 6 well plates (Thermo Fisher Scientific) and when confluent, were differentiated in MEMα Medium Glutamax™ supplemented with 15% KnockOut™ SR (Invitrogen) for 7 days at 37°C under 5% CO_2 (Wolins et al., 2006). Adipogenic differentiation was imaged by using the transmission channel of the ZOE™ Fluorescent Cell Imager (Bio-Rad).

BM hematopoietic progenitor cells (HPs) purification and co-culture with 3T3-F442A or OP9 -differentiated adipocytes: Mature MKs from BM cells were defined as the population of cells generated using the methodology of the Frampton and Shivdasani laboratories (Dumon et al., 2006; Lecine et al., 1998). BM cells were flushed from femora and tibiae of 10-20 weeks-aged C57BL6/J male mice. The cells were spun down and resuspended in ACK buffer (0.15M NH_4Cl; 1mM $KHCO_3$; 0.1mM Na_2EDTA pH 7.3) for 5 minutes to lyse mature erythrocytes. After filtration using easy strainer™ 70 µm and centrifugation 300xg for 5 minutes, the pelleted cells were resuspended in DMEM Glutamax™ (Invitrogen) supplemented with 10% fetal bovine serum (Invitrogen) and 100UI/mL penicillin/100µg/mL streptomycin (Sigma-Aldrich). Lineage cell (Lin^+ cell) depletion was further performed by

incubating cells with antibodies against CD16/CD32 (BD Pharmingen™), Gr1 (eBioscience™), B220 (BD Pharmingen™) and CD11b (eBioscience™) for 30 minutes on ice, followed by incubation with sheep anti-rat IgG immunomagnetic Dynabeads (Invitrogen). Two cycles of centrifugation (300x*g* for 5 minutes at 4°C) and resuspension were performed to allow bead-antibody interaction. The use of a magnet enabled collection of non-bound cells in the supernatant. The remaining Lin^- cells (called HPs) were then centrifuged and resuspended at $2x10^6$ cells/mL in 10% serum-supplemented DMEM Glutamax™ and 100UI/mL penicillin/100µg/mL streptomycin. 1mL of cells was seeded in the upper chamber of the 0.4 µm cell culture insert of 30mm diameter (Transwell chamber, Merck Millipore) over adherent 3T3-F442A or OP9 -differentiated adipocytes (no direct contact) at 37°C under 5% CO_2 in the presence of recombinant mouse TPO (50ng/mL, Peprotech) for 4 days to induce HP differentiation into MKs. Isolation of mature MKs was carried out on a bovine serum albumin (BSA) gradient (1.5%/3%) under gravity (1x*g*) for 40 minutes at room temperature.

Preparation of murine washed platelets: Whole blood was drawn from the inferior vena cava of anesthetized mice with a mixture of Imalgene (25mg/kg) (Merial) and Rompun (10 mg/kg) (Bayer) into a syringe containing acid citrate dextrose (3% trisodium citrate x5.5H20, 1.4% citric acid, 2% glucose) (1 anticoagulant volume / 9 blood volumes). Platelet-rich plasma (PRP) was obtained by mixing blood with 1 volume of modified HEPES-Tyrode's buffer (140mM NaCl, 2mM KCl, 12mM $NaHCO_3$, 0.3mM NaH_2PO_4, 1M $MgCl_2$, 5.5mM glucose, 5mM HEPES, pH 6.7) containing 0.35% BSA followed by a 300x*g* centrifugation for 4 minutes. After PGI_2 (Sigma-Aldrich) addition at a final concentration of 500nM to the PRP, platelets were pelleted by centrifugation at 1,000x*g* for 6 minutes and resuspended in modified HEPES-Tyrode's buffer (pH 7.38) in the presence of 0.02IU/mL of the ADP

(adenosine-5′-triphosphate diphosphohydrolase) scavenger apyrase (Sigma-Aldrich) and rested for 45 minutes at 37°C.

METHOD DETAILS

Flow cytometry: CD41-CD42b double expression was analyzed on HPs/MKs stained with both FITC-conjugated anti–mouse CD41 (BD Pharmingen™) and PE-conjugated anti–mouse CD42b (Emfret ANALYTICS) antibodies in PBS-1% BSA for 30 minutes at room temperature. Cell survival was analyzed after labeling of HPs/MKs with an anti-annexin V antibody (BD Pharmingen™) in Binding Buffer (10mM Hepes (pH 7.4), 140mM NaCl, 2.5mM $CaCl_2$) for 30 minutes at room temperature. Fresh cell samples were further analyzed on an LSRFortessa™ Cell analyzer flow cytometer (BD Biosciences) and Diva software (BD Biosciences). DNA content analysis was performed in MKs isolated from a BSA gradient. After fixation with 0.5 % formaldehyde on ice for 30 minutes, MKs were stained with a staining solution containing 2mM $MgCl_2$, 0.05% saponin, 10µg/mL propidium iodide (Invitrogen) and 10U/mL RNAse A (Roche) for 2 hours at 4°C and immediately analyzed by using an LSRFortessa™ Cell analyzaer flow cytometer and Diva software.

Transmission electron microscopy: Mature MKs after BSA gradient or washed platelets were fixed at 4°C for 24 hours in a buffer containing 2.5% glutaraldehyde, 0.05M sodium cocadylate and 1% glucose. Pieces of freshly flushed BM from mice tibiae were fixed with 2% glutaraldehyde in 0.1M Sorensen's phosphate buffer (pH 7.4). Samples were mixed in 2% agarose and cut in 1mm pieces whereas BM pieces were embedded in 1% agarose and kept whole. Samples were post-fixed with 1% osmium tetroxide in 0.2M sodium cacodylate buffer or in 0.05M Sorensen's phosphate buffer with 250mM glucose respectively for 1 hour at room temperature. Samples were then dehydrated in a series of graded ethanol solutions (30%/50%/70% 10 minutes each at room temperature) and embedded in Embed 812 resin

(Electron Microscopy Sciences) using a Leica EM AMW automated microwave tissue processor for electron microscopy. Finally, tissues were sliced into 70nm thick sections (Ultracut Reichert Jung) and mounted on 100-mesh collodion-coated copper grids prior to staining with 3% uranyle acetate in 50% ethanol and Reynold's lead citrate. Examinations were carried out on a Hitachi HT7700 transmission electron microscope at an accelerating voltage of 80 kV.

In situ BM and spleen staining: For histology, mouse tibiae or spleen were fixed with 10% formaldehyde for 24 hours and incubated at 4°C in 70% ethanol until paraffin embedding and chopped into 5µm thick sections. Paraffin was removed with Histoclear (Electron Microscopy Sciences) treatment and sections were hydrated by successive ethanol incubations (100/70/50/30%). Then, sections were successively stained with hematoxylin (Sigma-Aldrich) for 15 minutes and eosin (Sigma-Aldrich) for 30 seconds. After dehydratation with successive ethanol incubations (30/50/70/100%), sections were mounted. Images of the entire slice was performed with NanoZoomer 2.0 RS (Hamamatsu) and then manually analyzed with NDP view 2 (Hamamatsu) and ImageJ® software. For fluorescent immunostaining, mouse tibiae were fixed with 4% formaldehyde and 5mM sucrose for 24 hours and dehydrated with a graded sucrose serie (10/20/30%) for 3 days at 4°C. Subsequently, samples were embedded in OCT matrix (CellPath) and shock-frozen in liquid nitrogen. Five-micrometer–thick cryosections were probed with rabbit anti-human von Willebrand factor (vWF) (DAKO) antibody to specifically label MKs and platelets and mouse/rat anti-mouse FABP4/A-FABP antibody (R&DSystems) to stain microvascular endothelial cells (Cataltepe et al., 2012), followed by Alexa Fluor secondary antibodies. Nuclei were stained by using 4′,6-diamidino-2-phenylindole (DAPI, Sigma-Aldrich). Samples were visualized with an LSM780 confocal microscope operated with Zen software (Carl Zeiss) using a 63×, 1.4 numerical aperture Plan-

Apochromatic objective lens (Carl Zeiss). Image analysis was performed by using ImageJ software.

Triglyceride measurement: 3T3-F442A, OP9 and BM triglyceride content were measured by colorimetric technique using F6428 and T2449 kits according to manufacturer instructions (Sigma-Aldrich).

CFU fibroblast (CFU-F) assays. Cells were seeded at a clonal density of 16 cells/cm^2 in T-25 cm^2 flasks (Dutscher) in DMEM Glutamax™ (Invitrogen) supplemented with 10% fetal bovine serum (Invitrogen) and 100UI/mL penicillin/100µg/mL streptomycin (Sigma-Aldrich) for 3T3-F442A cells or in MEMα Medium Glutamax™ (Invitrogen) supplemented with 20% fetal bovine serum and 100UI/mL penicillin/100µg/mL streptomycin (Sigma-Aldrich) for OP9 cells at 37°C under 5% CO_2. After 10 days, the cells were gently washed with PBS and cell colonies were scored with the transmission channel of the ZOE™ Fluorescent Cell Imager (Bio-Rad). Cells from colonies were then dissociated by using Trypsin EDTA (Sigma-Aldrich) incubation during 5 minutes at 37°C under 5% CO_2 and replated in one well of TPP tissue culture Testplate 6 wells (TPP®) in DMEM Glutamax™ supplemented with 10% fetal bovine serum and penicillin/streptomycin in presence of 50nM insulin (Sigma-Aldrich) for 3T3-F442A cells or in one well of Nunclon™ Delta Surface 6 well plates (Thermo Fisher Scientific) in MEMα Medium Glutamax™ supplemented with 15% KnockOut™ SR (Invitrogen) and 100UI/mL penicillin/100µg/mL streptomycin (Sigma-Aldrich) for OP9 cells for 7 days at 37°C under 5% CO_2. Adipogenic differentiation was imaged by using the transmission channel of the ZOE™ Fluorescent Cell Imager (Bio-Rad).

Red oil staining of adipocytes: After fixation with 10% formaldehyde for 20 minutes, adipocytes were washed with 60% isopropanol and further labeled with 0.35 % Red oil (Sigma-Aldrich) for 20 minutes. Red oil labeling was visualized by using the inverted Nikon

Eclipse Ti microscope and NIS-Elements AR software, and quantified by using ImageJ® software as the percentage of the field labeled with Red oil.

Proplatelet formation assays: The analysis of the dynamics of platelet formation from BM explants was performed as previously described (Strassel et al., 2012). Briefly, after flushing, 0.5-1mm sections of marrow were maintained in Tyrode's buffer (0.137M NaCl, 2.68mM KCl, 11.9mM $NaHCO_3$, 0.4mM NaH_2PO_4, 1mM $MgCl_2$, 2mM $CaCl_2$, 5mM HEPES, 0.35% BSA, 5% mouse serum at pH=7.3) with 15IU/mL heparin in a 5% humidified CO_2 atmosphere at 37 °C. Cells were left to migrate out of the explants for 2 hours prior to imaging. Videomicroscopy was performed with an Axio Observer.Z1 microscope operated by the Zen software (Carl Zeiss) in a controlled atmosphere for 15 hours. Images were taken every 5 minutes with an ORCA R2 camera (Hamamatsu) using a 10×, 0.30 EC Plan-Neofluar lens (Carl Zeiss). A motorized multi-position stage (in *x*, *y*, *z*) was used, and an average of 150 stage positions, randomly picked showing 1–2 MKs per field, were followed. Proplatelet formation was quantified manually using Zen software as the percentage of alive MKs that extend proplatelets in a given time point. *In vitro* proplatet formation analysis was performed by plating for 6 hours on a fibrinogen matrix (100µg/mL) *in vitro* differentiated MKs and isolated by BSA gradient. The percentage of proplatelet forming MKs was manually quantified by using the transmission channel of the ZOE™ Fluorescent Cell Imager (Bio-Rad).

Real-Time PCR: Total RNAs were isolated by using GeneElute Mammalian Total RNA Miniprep Kit (Sigma-Aldrich). Total RNAs (500ng) were reverse transcribed using High Capacity cDNA reverse transcription kit (Applied Biosystems) in the presence of random hexamers. Real-time PCR was performed on 6.25ng cDNA and 100–900nmol/L specific oligonucleotide primers (see Key Resources Table) in a final volume of 10µL using the MESA Blue qPCR™ Mastermix for SYBR® Assay (Eurogentec). Fluorescence was

monitored and analyzed in a StepOnePlus Real-Time PCR system instrument (Applied Biosystems™). Minus reverse transcriptase (RT-) reaction was performed to ensure the absence of genomic DNA contamination and β2 microglobulin was used to normalize gene expression. Results are expressed as fold change to the following formula: $2^{(-\Delta\Delta Ct)}$ or as % to the following formula : $2^{(-\Delta\Delta Ct)}$ x100 where Ct corresponds to the number of cycles needed to generate a fluorescent signal above a predefined threshold and ΔΔCt corresponds to (Ctgene-Ctβ2microglobulin of the interest condition) – (Ctgene-Ctβ2microglobulin of the reference condition).

Fatty acid uptake: Confluent mouse 3T3-F442A pre-adipocyte or OP9 cells were differentiated into adipocytes in presence of ^{14}C palmitic acid (0.12µCi/mL) (Perkin Elmer) or Bodipy™ C12 (1µg/mL) (Invitrogen) for 7 days. Labeled adipocytes were therefore co-cultured with MKs. After 4 days, radioactivity was counted in MKs, adipocytes and supernatant by using a TRI-CARB 2100TR Liquid Scintillation Counter (Perkin Elmer) or fluorescence was visualized in MKs by confocal microscopy using a LSM780 operated with Zen software using a 63x, 1.4 NA Plan Apochromatic objective lens (Carl Zeiss).

Lipid analysis: After co-culture with ^{14}C palmitic acid -labeled adipocytes, lipids were immediately extracted by the modified procedure of Bligh and Dyer and resolved on thin layer chromatography (TLC) Silica Gel 60 (Merck Millipore) in chloroform/methanol/acetic acid/water (65:43:1:3, by vol.) solution. Spots corresponding to different lipids were then scraped off and ^{14}C palmitic acid was immediately analyzed in different lipids by using a TRI-CARB 2100TR Liquid Scintillation Counter (Perkin Elmer).

Cell lysis and protein quantification: Adipocytes or MKs from 1 well of co-culture plates were lysed in 50µL of lysis buffer (20mM Tris-HCl, pH 7.5, 150mM NaCl, 1mM EGTA, 4mM EDTA, 1% Triton X100, 0.2% SDS, 1mM PMSF, 1mM Na_3VO_4, 1µg/mL leupeptin,

1µg/mL aprotinin) during 30 minutes at 4°C under agitation. Samples were sonicated 2 times for 30 seconds at 30% amplitude at 4°C and cell debris were removed by centrifugation at 10,000×*g* for 15 minutes at 4°C. Aqueous phase was collected and submitted to a protein assay by using Protein quantitation kit BC assay (Interchim). Samples were standardized at 1µg/µL with lysis buffer and reducing Laemmli sample buffer containing 100mM Tris-HCl (pH 6.8), 15% (v/v) glycerol, 25mM DTT and 3% SDS and boiled for 5 minutes at 95°C.

Gel electrophoresis and immunoblotting: 20µg of protein samples were loaded on 10% polyacrylamide gel. Proteins were separated by SDS-PAGE, transferred on a nitrocellulose membrane (Gelman Sciences) and analyzed using the relevant antibody. The membrane was blocked using 3% BSA in Tris-Buffer-Saline containing 0.1% Tween (TBST) for 60 minutes. Membranes were probed overnight with the respective primary antibody (see Key Resources Table). After washing with TBST, the blots were probed with HRP-tagged secondary antibodies and washed again. Signals were detected using Clarity/Clarity Max™ Western ECL substrate (Bio-Rad) and Chemidoc Imaging system (Bio-Rad) The bands were quantified using ImageLab software (Bio-Rad) and normalized to the corresponding total protein loading.

Flow assay on collagen: Biochips microcapillaries (Vena8 Fluoro+, Cellix) were coated with a fibrillar collagen suspension (50µg/mL) for 1 hour and saturated with a solution of 0.5% BSA. Whole blood was drawn from the inferior vena cava of anesthetized mice with a mixture of Imalgene (25mg/kg) (Merial) and Rompun (10mg/kg) (Bayer) into a syringe containing heparin (10IU/mL) (1 volume anticoagulant / 9 volumes blood). Platelets were labeled with $DIOC_6$ (2µM, Invitrogen) in whole blood for 10 minutes at 37°C. Using a syringe pump (PHD-2000, Harvard Apparatus) labeled blood was perfused through a microcapillary for 2 minutes at different wall shear rate at 37°C. Platelet adhesion and thrombus formation were visualized with a 40x oil immersion objective for both fluorescent

and transmitted light microscopy and recorded in real time (1 frame every 5 seconds) with ORCA Camera (Carl Zeiss). Image sequences of the time lapse recording and analysis of surface coverage were performed offline on single frame by quantification of pixel surface after manual thresholding using ImageJ® software. Thrombi volumes are calculated by thresholding of surface covered by thrombi on slice of Z-stack images and addition of voxel (automatically converted into μm^3 by Zeiss software).

Immune-induced thrombocytopenia: Thrombocytopenia was induced by intraperitoneal injection of anti-mouse GPIbα antibody (2 μg/g, Emfret ANALYTICS). Blood samples were collected by tail bleeding at different times and platelet counts were measured using ABX Micros 60 analyser (HORIBA Medical).

Platelet lifespan: Circulating platelets were labeled in vivo by mice intravenous injection of $Dylight^{488}$-anti-GPIbβ Ig derivative (0.1 μg/g, Emfret ANALYTICS). 2 hours after antibody injection and every 24 hours for 4 days, the percentage of the $Dylight^{488}$-positive platelet population in whole blood from tail bleeding was determined using an LSRFortessaTM Cell analyser flow cytometer and Diva software (BD Biosciences).

Tail bleeding time. 3mm tail-tip transection in mice anesthetized by an intra-peritoneal injection of a mixture of Imalgene (25mg/kg) (Merial) and Rompun (10mg/kg) (Bayer). A stopwatch was started immediately upon transection to determine the time required for the bleeding to stop. Blood drops were removed every 15 seconds with the use of a paper filter. If bleeding did not recur within 30 seconds of cessation, it was considered stopped.

QUANTIFICATION AND STATISTICAL ANALYSIS

Data are expressed as mean±SD. Significance of differences, mentioned in the figure legend, was determined by using Prism6 (GraphPad software). p values < 0.05 were considered

significant (*p<0.05, **p<0.01, ***p<0.001) using unpaired two-tailed Student, one-sample t test, one-way ANOVA with the Tukey post hoc test or two-way ANOVA with Bonferroni post hoc test.

References

Adler, B.J., Green, D.E., Pagnotti, G.M., Chan, M.E., and Rubin, C.T. (2014a). High fat diet rapidly suppresses B lymphopoiesis by disrupting the supportive capacity of the bone marrow niche. PloS one *9*, e90639.

Adler, B.J., Kaushansky, K., and Rubin, C.T. (2014b). Obesity-driven disruption of haematopoiesis and the bone marrow niche. Nature reviews Endocrinology *10*, 737-748.

Ambrosi, T.H., Scialdone, A., Graja, A., Gohlke, S., Jank, A.M., Bocian, C., Woelk, L., Fan, H., Logan, D.W., Schurmann, A.*, et al.* (2017). Adipocyte Accumulation in the Bone Marrow during Obesity and Aging Impairs Stem Cell-Based Hematopoietic and Bone Regeneration. Cell stem cell *20*, 771-784 e776.

Asada, N., Takeishi, S., and Frenette, P.S. (2017). Complexity of bone marrow hematopoietic stem cell niche. Int J Hematol *106*, 45-54.

Attane, C., Esteve, D., Chaoui, K., Iacovoni, J.S., Corre, J., Moutahir, M., Valet, P., Schiltz, O., Reina, N., and Muller, C. (2020). Human Bone Marrow Is Comprised of Adipocytes with Specific Lipid Metabolism. Cell Rep *30*, 949-958 e946.

Bonner, J.C. (2004). Regulation of PDGF and its receptors in fibrotic diseases. Cytokine Growth Factor Rev *15*, 255-273.

Boucher, J., Masri, B., Daviaud, D., Gesta, S., Guigne, C., Mazzucotelli, A., Castan-Laurell, I., Tack, I., Knibiehler, B., Carpene, C.*, et al.* (2005). Apelin, a newly identified adipokine up-regulated by insulin and obesity. Endocrinology *146*, 1764-1771.

Cataltepe, O., Arikan, M.C., Ghelfi, E., Karaaslan, C., Ozsurekci, Y., Dresser, K., Li, Y., Smith, T.W., and Cataltepe, S. (2012). Fatty acid binding protein 4 is expressed in distinct endothelial and non-endothelial cell populations in glioblastoma. Neuropathol Appl Neurobiol *38*, 400-410.

Cawthorn, W.P., Scheller, E.L., Learman, B.S., Parlee, S.D., Simon, B.R., Mori, H., Ning, X., Bree, A.J., Schell, B., Broome, D.T., *et al.* (2014). Bone marrow adipose tissue is an endocrine organ that contributes to increased circulating adiponectin during caloric restriction. Cell metabolism *20*, 368-375.

Chagraoui, H., Komura, E., Tulliez, M., Giraudier, S., Vainchenker, W., and Wendling, F. (2002). Prominent role of TGF-beta 1 in thrombopoietin-induced myelofibrosis in mice. Blood *100*, 3495-3503.

Coort, S.L., Willems, J., Coumans, W.A., van der Vusse, G.J., Bonen, A., Glatz, J.F., and Luiken, J.J. (2002). Sulfo-N-succinimidyl esters of long chain fatty acids specifically inhibit fatty acid translocase (FAT/CD36)-mediated cellular fatty acid uptake. Mol Cell Biochem *239*, 213-219.

Craft, C.S., Li, Z., MacDougald, O.A., and Scheller, E.L. (2018). Molecular differences between subtypes of bone marrow adipocytes. Curr Mol Biol Rep *4*, 16-23.

Davizon-Castillo, P., McMahon, B., Aguila, S., Bark, D., Ashworth, K., Allawzi, A., Campbell, R.A., Montenont, E., Nemkov, T., D'Alessandro, A., *et al.* (2019). TNF-alpha-driven inflammation and mitochondrial dysfunction define the platelet hyperreactivity of aging. Blood *134*, 727-740.

Dhenge, A., Limbkar, K., Melinkeri, S., Kale, V.P., and Limaye, L. (2017). Arachidonic acid and Docosahexanoic acid enhance platelet formation from human apheresis-derived CD34(+) cells. Cell Cycle *16*, 979-990.

do Carmo, L.S., Rogero, M.M., Paredes-Gamero, E.J., Nogueira-Pedro, A., Xavier, J.G., Cortez, M., Borges, M.C., Fujii, T.M., Borelli, P., and Fock, R.A. (2013). A high-fat diet increases interleukin-3 and granulocyte colony-stimulating factor production by bone marrow cells and triggers bone marrow hyperplasia and neutrophilia in Wistar rats. Exp Biol Med (Maywood) *238*, 375-384.

Doucette, C.R., Horowitz, M.C., Berry, R., MacDougald, O.A., Anunciado-Koza, R., Koza, R.A., and Rosen, C.J. (2015). A High Fat Diet Increases Bone Marrow Adipose Tissue (MAT) But Does Not Alter Trabecular or Cortical Bone Mass in C57BL/6J Mice. Journal of cellular physiology *230*, 2032-2037.

Dumon, S., Heath, V.L., Tomlinson, M.G., Gottgens, B., and Frampton, J. (2006). Differentiation of murine committed megakaryocytic progenitors isolated by a novel strategy reveals the complexity of GATA and Ets factor involvement in megakaryocytopoiesis and an unexpected potential role for GATA-6. Experimental hematology *34*, 654-663.

Fruhbeck, G., Mendez-Gimenez, L., Fernandez-Formoso, J.A., Fernandez, S., and Rodriguez, A. (2014). Regulation of adipocyte lipolysis. Nutr Res Rev *27*, 63-93.

Ge, Q., Ryken, L., Noel, L., Maury, E., and Brichard, S.M. (2011). Adipokines identified as new downstream targets for adiponectin: lessons from adiponectin-overexpressing or -deficient mice. American journal of physiology Endocrinology and metabolism *301*, E326-335.

Geddis, A.E. (2010). Megakaryopoiesis. Semin Hematol *47*, 212-219.

Guerrero, J.A., Bennett, C., van der Weyden, L., McKinney, H., Chin, M., Nurden, P., McIntyre, Z., Cambridge, E.L., Estabel, J., Wardle-Jones, H.*, et al.* (2014). Gray platelet syndrome: proinflammatory megakaryocytes and alpha-granule loss cause myelofibrosis and confer metastasis resistance in mice. Blood *124*, 3624-3635.

Hindorf, C., Glatting, G., Chiesa, C., Linden, O., Flux, G., and Committee, E.D. (2010). EANM Dosimetry Committee guidelines for bone marrow and whole-body dosimetry. Eur J Nucl Med Mol Imaging *37*, 1238-1250.

Horowitz, M.C., Berry, R., Holtrup, B., Sebo, Z., Nelson, T., Fretz, J.A., Lindskog, D., Kaplan, J.L., Ables, G., Rodeheffer, M.S.*, et al.* (2017). Bone marrow adipocytes. Adipocyte *6*, 193-204.

Karlsson, E.A., Sheridan, P.A., and Beck, M.A. (2010). Diet-induced obesity in mice reduces the maintenance of influenza-specific CD8+ memory T cells. The Journal of nutrition *140*, 1691-1697.

Laurent, V., Toulet, A., Attane, C., Milhas, D., Dauvillier, S., Zaidi, F., Clement, E., Cinato, M., Le Gonidec, S., Guerard, A.*, et al.* (2019). Periprostatic Adipose Tissue Favors Prostate Cancer Cell Invasion in an Obesity-Dependent Manner: Role of Oxidative Stress. Mol Cancer Res.

Lecine, P., Blank, V., and Shivdasani, R. (1998). Characterization of the hematopoietic transcription factor NF-E2 in primary murine megakaryocytes. J Biol Chem *273*, 7572-7578.

Li, Z., Hardij, J., Bagchi, D.P., Scheller, E.L., and MacDougald, O.A. (2018). Development, regulation, metabolism and function of bone marrow adipose tissues. Bone *110*, 134-140.

Machlus, K.R., and Italiano, J.E., Jr. (2013). The incredible journey: From megakaryocyte development to platelet formation. The Journal of cell biology *201*, 785-796.

Machlus, K.R., Thon, J.N., and Italiano, J.E., Jr. (2014). Interpreting the developmental dance of the megakaryocyte: a review of the cellular and molecular processes mediating platelet formation. British journal of haematology *165*, 227-236.

Malara, A., Abbonante, V., Di Buduo, C.A., Tozzi, L., Currao, M., and Balduini, A. (2015). The secret life of a megakaryocyte: emerging roles in bone marrow homeostasis control. Cell Mol Life Sci *72*, 1517-1536.

Malara, A., Abbonante, V., Zingariello, M., Migliaccio, A., and Balduini, A. (2018). Megakaryocyte Contribution to Bone Marrow Fibrosis: many Arrows in the Quiver. Mediterr J Hematol Infect Dis *10*, e2018068.

Malara, A., Currao, M., Gruppi, C., Celesti, G., Viarengo, G., Buracchi, C., Laghi, L., Kaplan, D.L., and Balduini, A. (2014). Megakaryocytes Contribute to the Bone Marrow-Matrix

Environment by Expressing Fibronectin, Type IV Collagen, and Laminin. Stem Cells *32*, 926-937.

Murphy, A.J., Bijl, N., Yvan-Charvet, L., Welch, C.B., Bhagwat, N., Reheman, A., Wang, Y., Shaw, J.A., Levine, R.L., Ni, H.*, et al.* (2013). Cholesterol efflux in megakaryocyte progenitors suppresses platelet production and thrombocytosis. Nat Med *19*, 586-594.

Naveiras, O., Nardi, V., Wenzel, P.L., Hauschka, P.V., Fahey, F., and Daley, G.Q. (2009). Bone-marrow adipocytes as negative regulators of the haematopoietic microenvironment. Nature *460*, 259-263.

Nielsen, T.S., Jessen, N., Jorgensen, J.O., Moller, N., and Lund, S. (2014). Dissecting adipose tissue lipolysis: molecular regulation and implications for metabolic disease. J Mol Endocrinol *52*, R199-222.

Nieman, K.M., Kenny, H.A., Penicka, C.V., Ladanyi, A., Buell-Gutbrod, R., Zillhardt, M.R., Romero, I.L., Carey, M.S., Mills, G.B., Hotamisligil, G.S.*, et al.* (2011). Adipocytes promote ovarian cancer metastasis and provide energy for rapid tumor growth. Nat Med *17*, 1498-1503.

Pepino, M.Y., Kuda, O., Samovski, D., and Abumrad, N.A. (2014). Structure-function of CD36 and importance of fatty acid signal transduction in fat metabolism. Annu Rev Nutr *34*, 281-303.

Pohlers, D., Brenmoehl, J., Loffler, I., Muller, C.K., Leipner, C., Schultze-Mosgau, S., Stallmach, A., Kinne, R.W., and Wolf, G. (2009). TGF-beta and fibrosis in different organs - molecular pathway imprints. Biochim Biophys Acta *1792*, 746-756.

Scheller, E.L., Cawthorn, W.P., Burr, A.A., Horowitz, M.C., and MacDougald, O.A. (2016). Marrow Adipose Tissue: Trimming the Fat. Trends in endocrinology and metabolism: TEM *27*, 392-403.

Scheller, E.L., Doucette, C.R., Learman, B.S., Cawthorn, W.P., Khandaker, S., Schell, B., Wu, B., Ding, S.Y., Bredella, M.A., Fazeli, P.K., *et al.* (2015). Region-specific variation in the properties of skeletal adipocytes reveals regulated and constitutive marrow adipose tissues. Nat Commun *6*, 7808.

Siddiqui, N.F., Shabrani, N.C., Kale, V.P., and Limaye, L.S. (2011). Enhanced generation of megakaryocytes from umbilical cord blood-derived CD34(+) cells expanded in the presence of two nutraceuticals, docosahexanoic acid and arachidonic acid, as supplements to the cytokine-containing medium. Cytotherapy *13*, 114-128.

Singer, K., DelProposto, J., Morris, D.L., Zamarron, B., Mergian, T., Maley, N., Cho, K.W., Geletka, L., Subbaiah, P., Muir, L., *et al.* (2014). Diet-induced obesity promotes myelopoiesis in hematopoietic stem cells. Molecular metabolism *3*, 664-675.

Strassel, C., Eckly, A., Leon, C., Moog, S., Cazenave, J.P., Gachet, C., and Lanza, F. (2012). Hirudin and heparin enable efficient megakaryocyte differentiation of mouse bone marrow progenitors. Exp Cell Res *318*, 25-32.

Travlos, G.S. (2006). Normal structure, function, and histology of the bone marrow. Toxicologic pathology *34*, 548-565.

Trottier, M.D., Naaz, A., Li, Y., and Fraker, P.J. (2012). Enhancement of hematopoiesis and lymphopoiesis in diet-induced obese mice. Proceedings of the National Academy of Sciences of the United States of America *109*, 7622-7629.

van den Berg, S.M., Seijkens, T.T., Kusters, P.J., Beckers, L., den Toom, M., Smeets, E., Levels, J., de Winther, M.P., and Lutgens, E. (2016). Diet-induced obesity in mice diminishes hematopoietic stem and progenitor cells in the bone marrow. FASEB J *30*, 1779-1788.

Wang, Y.Y., Attane, C., Milhas, D., Dirat, B., Dauvillier, S., Guerard, A., Gilhodes, J., Lazar, I., Alet, N., Laurent, V., *et al.* (2017). Mammary adipocytes stimulate breast cancer invasion through metabolic remodeling of tumor cells. JCI insight *2*, e87489.

Wickenhauser, C., Hillienhof, A., Jungheim, K., Lorenzen, J., Ruskowski, H., Hansmann, M.L., Thiele, J., and Fischer, R. (1995). Detection and quantification of transforming growth factor beta (TGF-beta) and platelet-derived growth factor (PDGF) release by normal human megakaryocytes. Leukemia *9*, 310-315.

Wolins, N.E., Quaynor, B.K., Skinner, J.R., Tzekov, A., Park, C., Choi, K., and Bickel, P.E. (2006). OP9 mouse stromal cells rapidly differentiate into adipocytes: characterization of a useful new model of adipogenesis. Journal of lipid research *47*, 450-460.

Yang, H., Youm, Y.H., Vandanmagsar, B., Rood, J., Kumar, K.G., Butler, A.A., and Dixit, V.D. (2009). Obesity accelerates thymic aging. Blood *114*, 3803-3812.

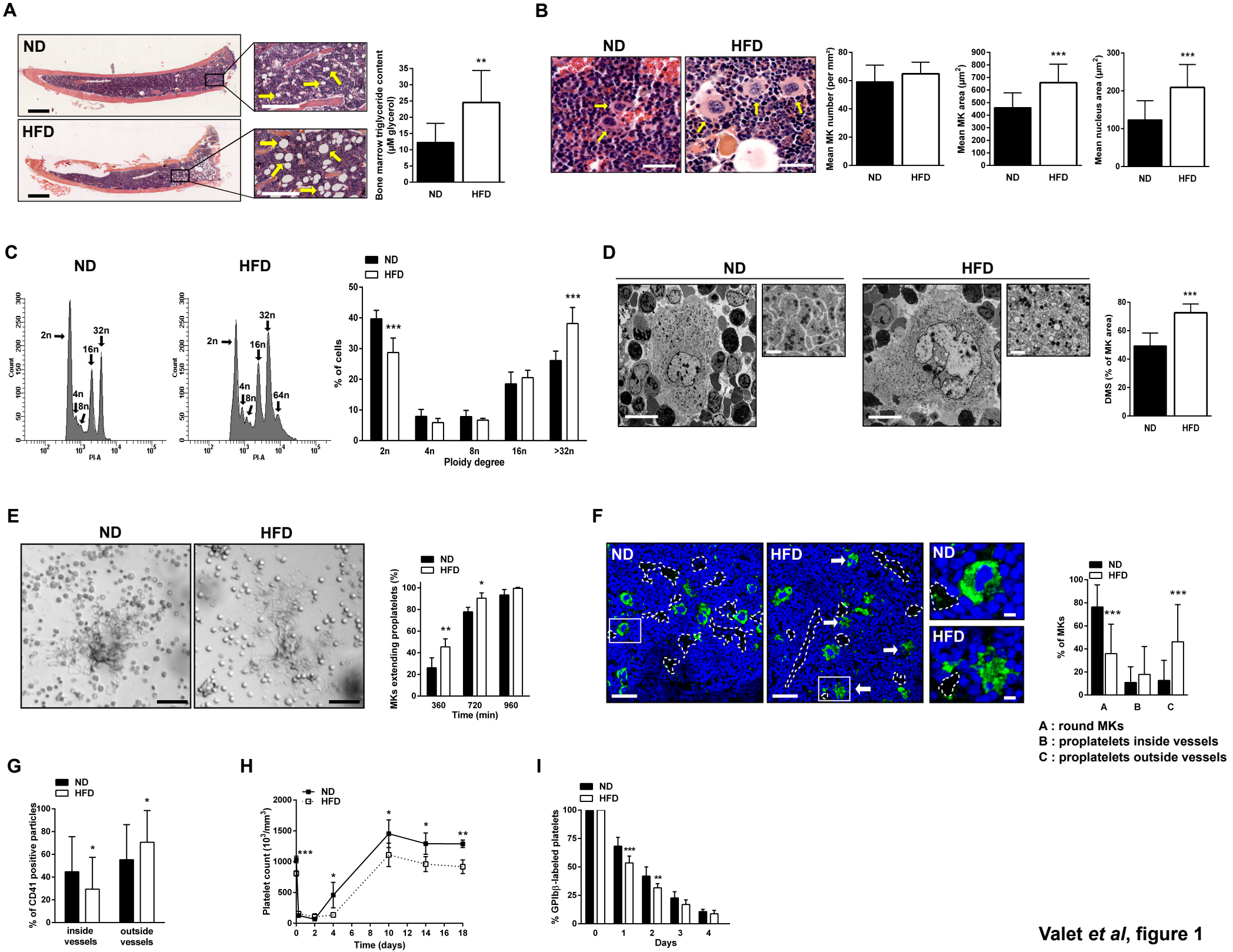

Valet *et al*, figure 1

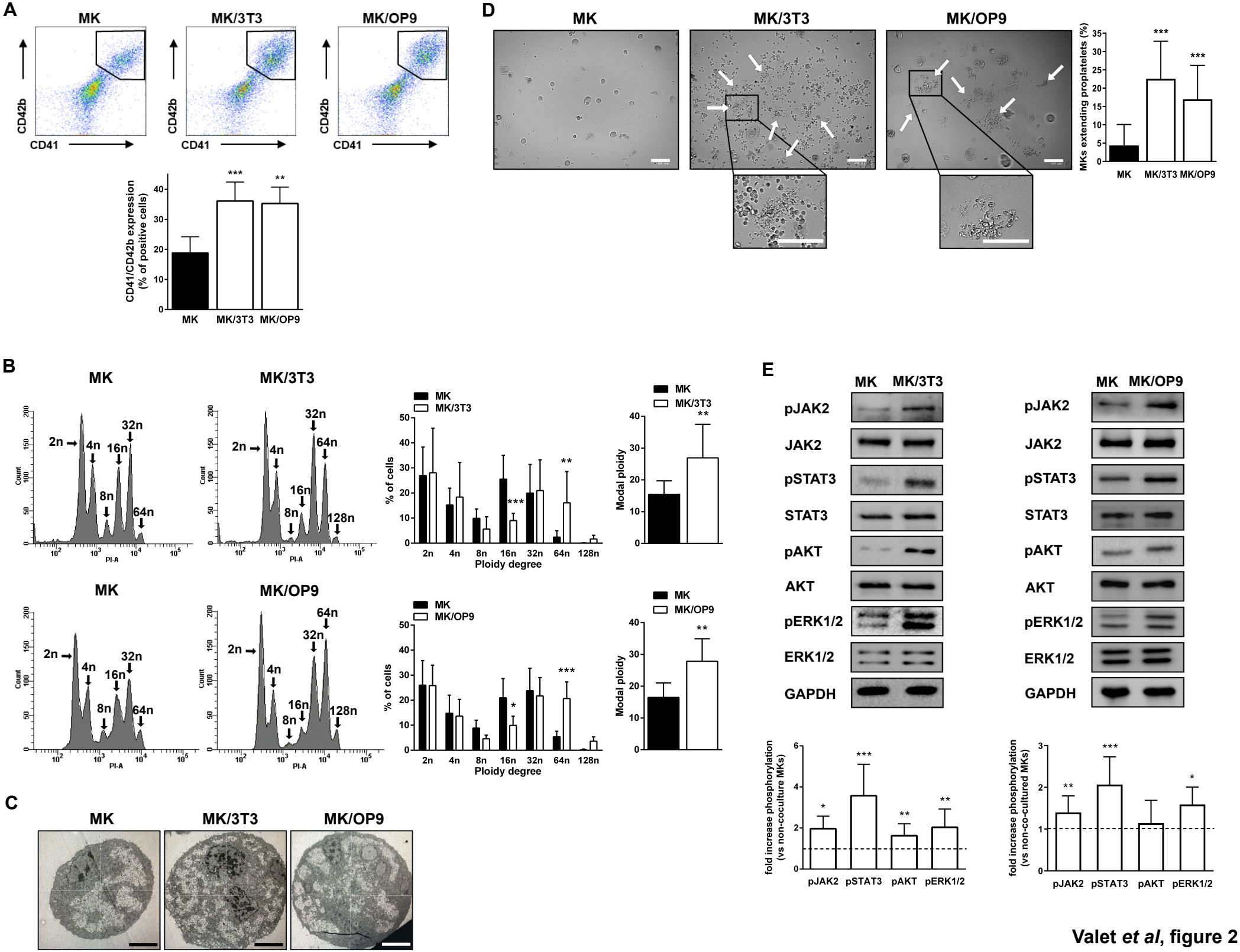

Valet *et al*, figure 2

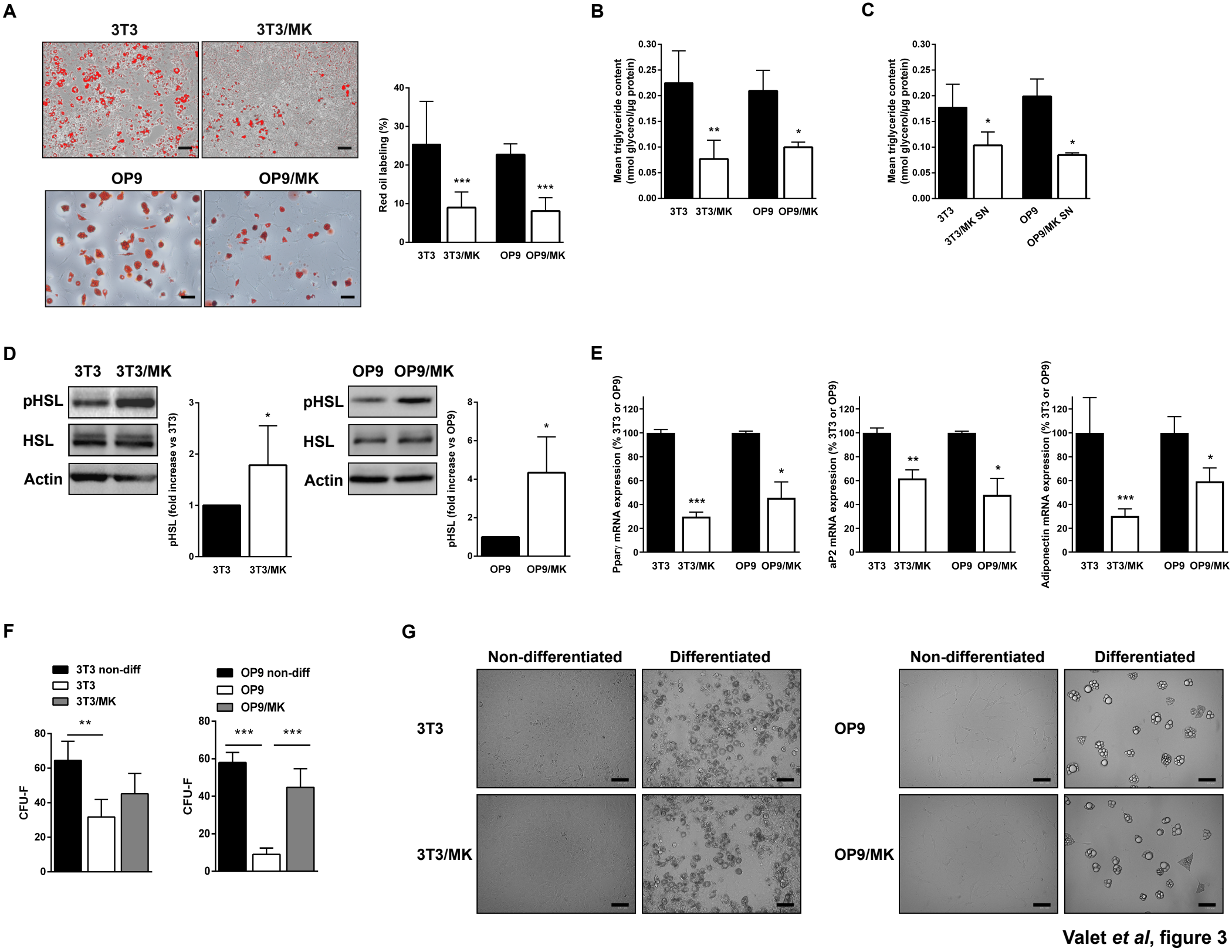

Valet *et al*, figure 3

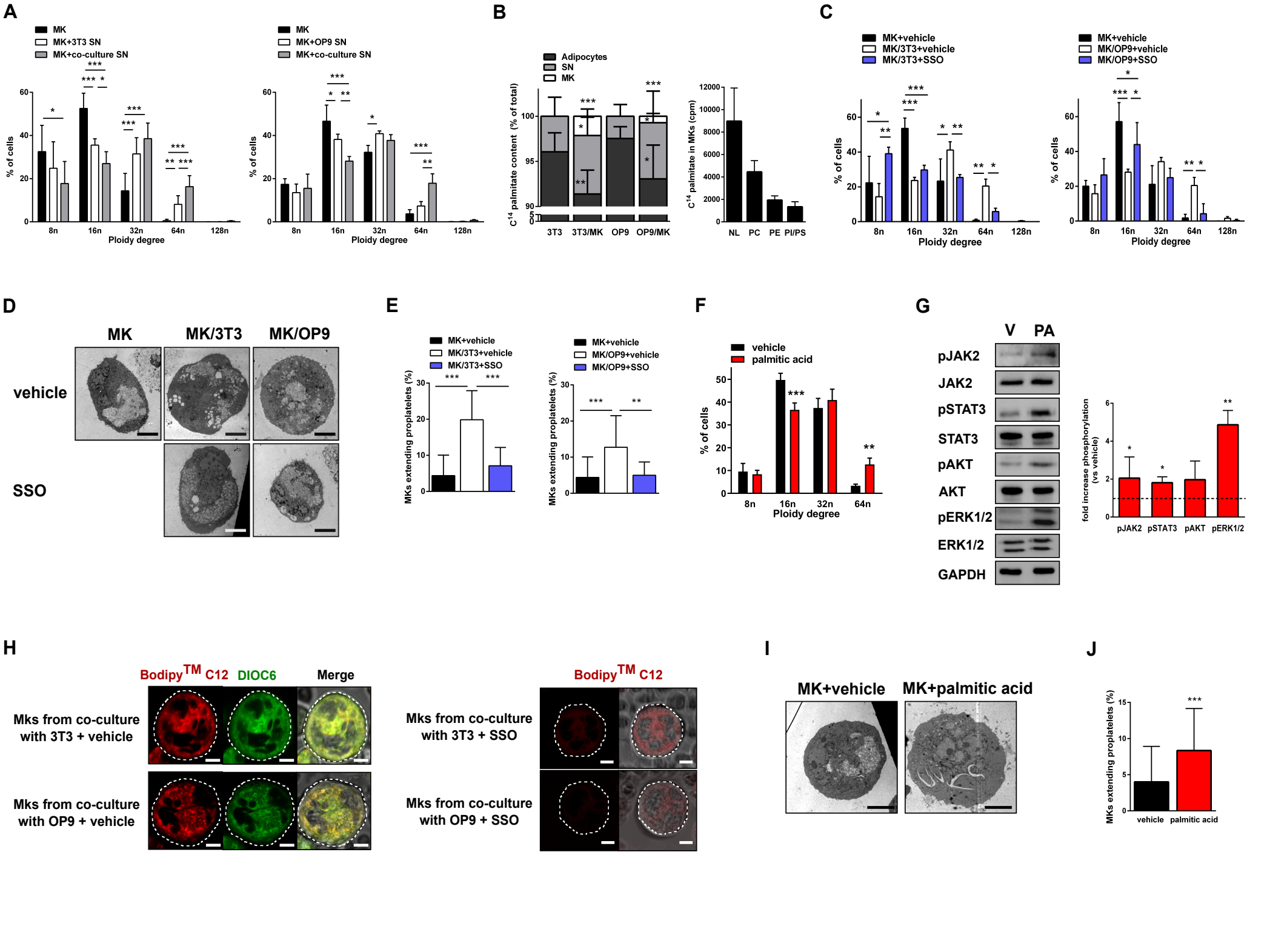

Valet et al, figure 4

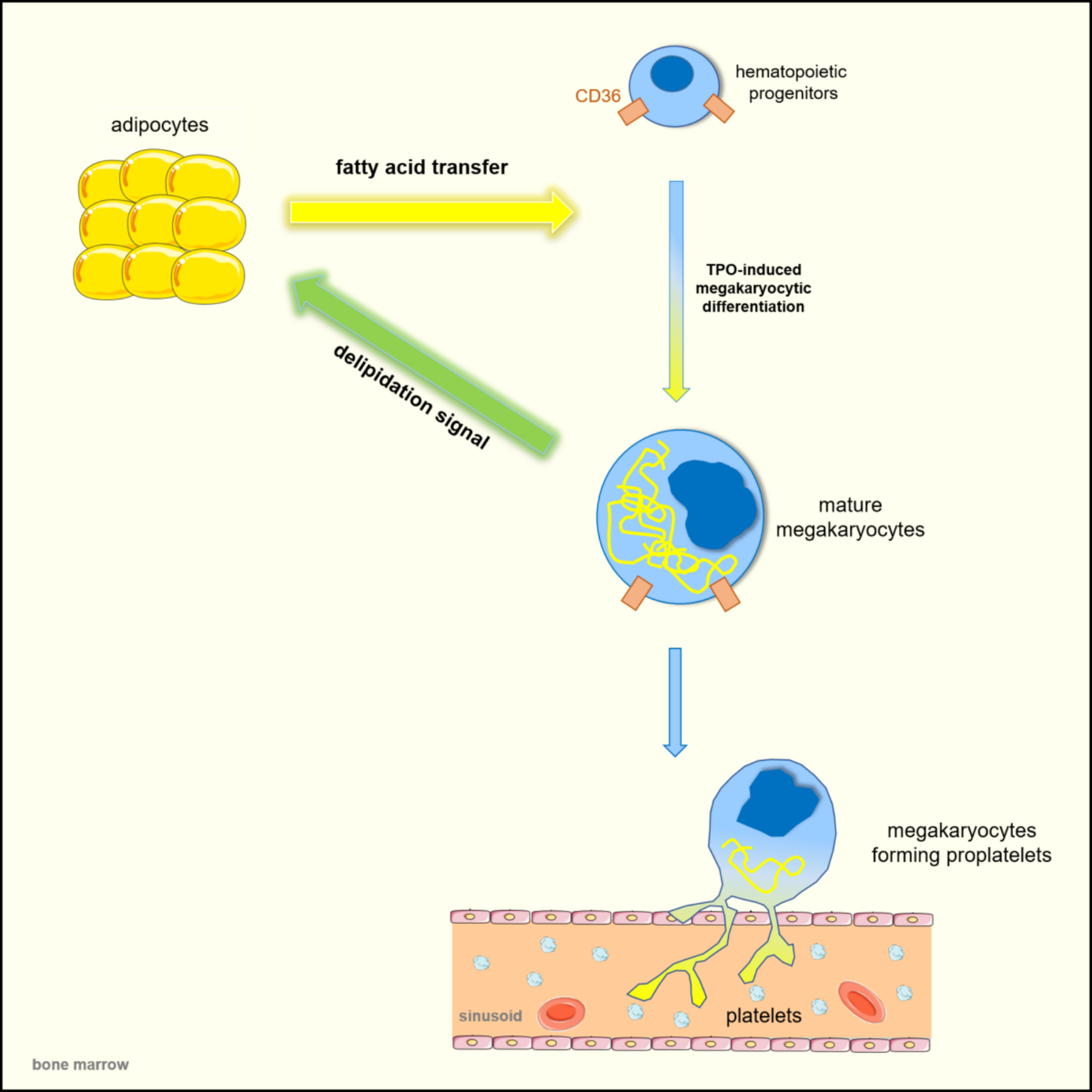
adipocytes
fatty acid transfer
CD36
hematopoietic progenitors
TPO-induced megakaryocytic differentiation
delipidation signal
mature megakaryocytes
megakaryocytes forming proplatelets
sinusoid
platelets
bone marrow